doi: 10.4149/gpb_2023015

Immunobiochemical profile of clear cell renal cell carcinoma (ccRCC): A preliminary study

Daniela Vargová[1], Ján Dargaj[2], Soňa Fraňová[1], Matúš Dohál[3], Ján Ľupták[2], Ján Švihra[2], Lukáš Briš[2], Marián Grendár[4] and Martina Šutovská[1]

[1] *Department of Pharmacology, Jessenius Faculty of Medicine in Martin, Comenius University in Bratislava, Martin, Slovakia*
[2] *Department of Urology, Jessenius Faculty of Medicine in Martin, Comenius University in Bratislava and University Hospital Martin, Slovakia*
[3] *Biomedical Centre Martin, Jessenius Faculty of Medicine in Martin, Comenius University in Bratislava, Martin, Slovakia*
[4] *Bioinformatic unit, Biomedical Center Martin, Jessenius Faculty of Medicine in Martin, Comenius University in Bratislava, Martin, Slovakia*

Abstract. Clear cell renal cell carcinoma (ccRCC) is the most common variant of RCC. It is an aggressive disease with an unfavorable prognosis. The rich immune infiltrates present in the tumor microenvironment (TME) of ccRCC produce various signaling molecules, especially cytokines, which primarily activate the Jak/STAT pathway and significantly influence tumor pathogenesis. STAT3 has a well-defined oncogenic character. Using multiplex assays and ELISA, we have measured the concentrations of 27 cytokines and STAT3 in tumor and healthy renal tissue from 16 patients with histologically verified ccRCC. We have detected significantly higher levels of G-CSF, IL-6, CXCL10, CCL3, and CCL4 in tumor tissue than in their healthy counterparts. There were significant differences in the levels of IL-1β and PDGF-BB between tumors of different nuclear grades (NG). Intratumoral IL-12p70 and IL-15 showed a significant positive correlation with intratumoral STAT3. The concentration of STAT3 in tumors was significantly lower than in the kidney. An increase in tumor STAT3 levels was associated with an increase in the pathological stage of the disease (TNM), but not with NG. The results of our study confirm the significant role of various cytokines and STAT3 in the pathogenesis of ccRCC and indicate their clinical relevance.

Key words: Renal cell carcinoma — Cytokines — STAT3 — Tumor — Immune system

Introduction

Renal cell carcinoma (RCC), a tumor arising from renal cortical tubular cells, is the most common type of primary kidney cancer (80–85%) (Garfield 2021). From more than 10 different histological variants, clear cell RCC (ccRCC) is diagnosed most frequently (Vuong et al. 2019). On a global scale, RCC accounts for 2% of all oncologic diagnoses and deaths. However, in recent years, the incidence of RCC in developed countries has been increasing (Padala et al.

Electronic supplementary material. The online version of this article (doi: 10.4149/gpb_2023015) contains Supplementary material.
Correspondence to: Daniela Vargová, Department of Pharmacology, Jessenius Faculty of Medicine, Comenius University in Bratislava, Martin, Slovakia
E-mail: vargova238@uniba.sk
Ján Dargaj, Department of Urology, Jessenius Faculty of Medicine in Martin, Comenius University in Bratislava and University Hospital Martin, Slovakia
E-mail: jano.dargaj@gmail.com

2020). Typical symptoms such as hematuria, flank pain, and palpable mass are sporadic and occur in about 10% of all patients, and no screening test is currently available in clinical practice (Padala et al. 2020). Therefore, the majority of all cases are discovered incidentally, and one-third of patients, at the time of diagnosis, are in a locally advanced (pT3) or even metastatic (pT4) stage (Cairns 2011; Padala et al. 2020). The prognosis of this cancer is unfavorable and is considered to have the highest mortality rate among all urological malignancies (Padala et al. 2020). Due to chemo and radioresistance, the only curative option for patients with clinically localized RCC is nephrectomy. However, about 20–30% of patients with localized RCC will experience recurrence despite surgery (Mattila et al. 2021). Only 10% of patients in an advanced stage (pT4) reach 5-year survival (Kang et al. 2020). If untreated, the median survival of such patients ranges from 6 to 12 months (di Pietro et al. 2018).

RCC has a well-known immunogenic character and a dense vascular network (Heidegger et al. 2019). Inflammatory cells have been detected in the tumor microenvironment (TME) and play a crucial role in the pathogenesis of RCC (Zhang et al. 2019). TMEs are abundant in signaling molecules, namely cytokines. Cytokines have pleiotropic effects and can be produced not only by immune cells infiltrated in the tumor, but also by tumor and stromal cells. They primarily modulate the immune response and inflammation. Furthermore, they can interfere with tumorigenesis in various ways (Kartikasari et al. 2021). Some cytokines can promote tumor progression by directly increasing angiogenesis (*via* up-regulation of VEGF, bFGF, or CXCL12) or by recruiting immunosuppressive leukocytes such as Tregs and MDSCs (Nagarsheth et al. 2017). Others act in favor of the host by inhibiting angiogenesis or increasing the number of effector cells (Th1, NK and CD8+) in the TME (Nagarsheth et al. 2017). In our previous study, we identified several cytokines as pathologically relevant in the pathogenesis of ccRCC (Vargová et al. 2022).

In target cells, cytokines signal through different pathways, for example, Src, Smad, MAPK/Erk, PI3-K/Akt/mTOR (phosphatidyl inositol 3-kinase), but most importantly through JAK (Janus kinase)/STAT (Hirano et al. 2000). STATs (signal transducers and activators of transcription) represent a family of seven nonphosphorylated ubiquitously expressed proteins (STAT1, STAT2, STAT3, STAT4, STAT5a, STAT5b, and STAT6) localized under basal conditions in the cytoplasm as latent unphosphorylated proteins. Among them, STAT3 plays a prominent role in the pathogenesis of cancer. Aberrant activation of STAT3 occurs in more than 70% of human cancers, including RCC (Horiguchi et al. 2002; Guo et al. 2009; Santoni et al. 2015; Verhoeven et al. 2020). Upstream activators of STAT3 include interleukins (IL-6, IL-7, IL-9, IL-10, IL-11, IL-12, IL-15, IL17 and IL-22), interferons, growth factors (G-CSF, EGF, HGF, VEGF, and PDGF), as well as non-receptor tyrosine kinases (Mizoguchi 2012; Bautista 2019). Activated STAT3 acts as a transcription factor and modulates the expression of a broad array of target genes, e.g., pro-angiogenic factors (VEGF, HIF-1α, bFGF, and HGF), cell cycle regulators (cyclin D1, c-Myc, survivin), matrix metalloproteinase 2 (MMP2), and immunosuppressive cytokines (IL-6, IL-10, TGF-β) among others (Lee et al. 2019). As a consequence, STAT3 hyperactivation increases the rate of angiogenesis and promotes tumor cell proliferation and survival, as well as their ability to invade, disseminate, and escape immune surveillance (Lee et al. 2019). In fact, constitutive activation of STAT3 is positively correlated with a poor prognosis (Zou et al. 2020).

The present study attempted to determine: 1) the immune biochemical profile (levels of STAT3 and 27 pathologically relevant cytokines) of ccRCC and healthy kidney tissue; 2) potentially tumor-promoting and/or antitumor cytokines and their relationship to STAT3; and 3) changes in cytokine and STAT3 levels according to clinicopathological characteristics such as tumor node metastasis (TNM) stage and tumor nuclear grades (NG).

Materials and Methods

Samples

Tissue samples from a total of 16 patients (3 women (19%) and 13 men (81%)) with histologically verified ccRCC were analyzed. Average age of female and male patients expressed as mean ± SD was 58.3 ± 7.5 and 61.2 ± 11.8 years, respectively. The range of age was 51–66 years and 46–86 years

Table 1. Distribution of patients according to gender, histopathological (NG), and clinical (TNM) disease stages

Gender	NG1	NG2	NG3	NG4	TNM 1	TNM 2	TNM 3	TNM 4
women	0	2	1	0	1	0	2	0
men	1	3	6	3	9	1	3	0
total (%)	1 (6.25)	5 (31.25)	7 (43.75)	3 (18.75)	10 (62.5)	1 (6.25)	5 (31.25)	0 (0)

NG, nuclear grading; TNM, tumor node metastasis staging system.

for women and men, respectively. The clinical and histopathological characteristics of a group of patients are summarized in Table 1. Patients suffering from any of the following: chronic inflammation of the urogenital system, systemic autoimmune disease, or rheumatological disease were excluded. Also, individuals undergoing any kind of anti-inflammatory or immunosuppressive therapy have not been included. Samples of tumor (T) and macroscopically healthy (normal, N) renal tissue were collected separately from the same kidney during nephrectomy at the Department of Urology of the Jessenius Faculty of Medicine, Comenius University and the Martin University Hospital. All samples were placed into sterile polypropylene tubes, transported immediately to the lab, and stored at −80°C until further processed.

Preparation of tissue homogenates

Two different types of tissue homogenates were prepared from each sample: one for the multiplex immunoassay and one for STAT3 detection by ELISA. The former were prepared using a Bio-Plex TM cell lysis kit (Bio-Rad, Hercules, California, USA) as follows: 100 mg of tissue was cut into pieces and rinsed with cell wash buffer (a part of the kit). The samples were then placed in a tube containing 500 µl of cell lysis solution (containing 99% of Cell Lysis Buffer; 0.4% of Factor 1; 0.2% of Factor 2, and 0.4% of 500 mM phenylmethylsulfonyl fluoride (PMSF) and homogenized on ice at 4000 rpm (Homogenizer Stuart SHM2/Euro, Bibby Scientific, UK). Finally, tissue lysates were centrifuged at 6805 rpm for 4 min at 4°C and the supernatant was collected, aliquoted, and frozen at −80°C until multiplex analysis. The supernatants for the ELISA were obtained similarly: 100 mg of tissue was minced on ice and rinsed with 0.02 M PBS (pH 7.0–7.2) to remove excess blood. The samples were then placed in 500 µl of 0.02 M PBS, homogenized (4000 rpm), centrifuged (7170 rpm for 5 min at 4°C), aliquoted, and frozen at −80°C.

Measurement of total protein (BCA protein assay)

The BCA assay (Thermo Scientific Pierce TM BCA Protein Assay) is a rapid, highly sensitive, precise, and detergent-compatible method for the colorimetric detection and quantification of the total protein concentration in a sample. It is a two-step reaction. First, cupric ions (Cu^{2+}) are reduced by proteins to cuprous ions (Cu^{1+}) in an alkaline medium containing sodium potassium tartrate (a process called the biuret reaction). Then, a blue-colored complex comprising one cuprous cation and two molecules of bicinchoninic acid (BCA) is formed. The intensity of this water-soluble complex is directly proportional to the level of proteins. Finally, the absorbances are evaluated by a multimode microplate reader, Varioskan TM LUX at 562 nm.

Assessment of cytokine and STAT3 levels in RCC and healthy kidney tissue

Cytokine concentrations were quantified using the Bio-Plex TM human cytokine standard 27-Plex assay (Bio-Rad, Hercules, California, USA). This 96-well plate-based analysis system allows us to detect 27 biologically relevant cytokines (basic fibroblast growth factor (bFGF), CXCL11 (eotaxin), granulocyte macrophage colony stimulating factor (GM-CSF), granulocyte colony stimulating factor (G-CSF); interferon gamma (IFN-γ); interleukins 1β, 1ra, 2, 4, 5, 6, 7, 8 (CXCL8), 9, 10, 12p70, 13, 15 and 17A; interferon gamma-induced protein 10 (IP-10/CXCL10); monocyte chemoattractant protein 1 (MCP-1/CCL2); macrophage inflammatory proteins 1 α and β/CCL3 and CCL4; platelet-derived growth factor-BB (PDGF-BB); RANTES (CCL5); tumor necrosis factor α (TNF-α), and vascular endothelial growth factor (VEGF)) simultaneously in each sample. The assay combines two approaches to detect the target molecules: sandwich ELISA and flow cytometry. First, the biomarker of interest reacts with capture antibodies coupled to magnetic beads. The unbound proteins are removed during a series of washes. Biotinylated antibodies are then added to each well and a sandwich complex is formed. Finally, the complex is labeled with the streptavidin-phycoerythrin (SA-PE) conjugate and is ready to be visualized. Visualization is performed using two laser lights from the built-in Bio-Plex® 200 System reader: the red one (635 nm) for identification of the bead region and the green one (532 nm) for quantifying the analytes. The data output is further processed by Bio-Plex Manager™ software. Cytokine levels are presented as median fluorescence intensity (MFI), and the final concentration, which is proportional to MFI, is expressed in pg/ml.

Sandwich ELISA (LS-F54989) was used for the detection of STAT3 tissue contents. The optical density (OD) of each sample was measured at 450 nm in the VarioskanTM LUX multimode microplate reader. The STAT3 concentration in each sample was calculated from the standard curve and expressed in pg/ml. The final concentrations (pg/mg) of both the cytokines and STAT3 in each sample were acquired after standardization with the total amount of protein measured by BCA.

Statistical analysis

The analysis of the acquired data was performed in R (R Core Team, 2021) ver. 4.0.5 with libraries rstatix (Kassambara 2021), ggpubr (Kassambara 2020), car (Fox 2019), and robustbase (Maechler 2021). The data were brought

close to normality using the logarithmic transformation suggested by the Symbox tool. The normality of the data was assessed using the quantile-quantile plot with the 95% confidence band constructed by bootstrap. After excluding gross outliers, the sample means and standard deviation (SD) were calculated. The transformed and cleaned log data were then visualized in a form of heatmap with the help of Metaboanalyst, a free online platform for metabolomic data analysis (https://www.metaboanalyst.ca/). To test the null hypothesis about the equality of population means in the tumor and native subpopulations, each variable was subjected to a paired *t*-test, and the effect size was quantified by Cohen's D. The probability of accepting an alternative hypothesis – *post hoc* statistical power was calculated using G power software (Faul et al. 2009). The null hypothesis about the equality of population means in subpopulations with different NG and clinical stages of TNM was tested by the Welch ANOVA test. If a finding was significant, pairwise Tukey-HSD comparisons were performed. The results of the paired *t*-test and the Welch ANOVA test were visualized by the combination of a box plot and a swarm plot. Next, robust regression was used to fit the linear regression model into log-STAT3 as a function of log cytokine (separately for tumor and native data). The effect size was quantified by Adjusted R2 and the correlation between log-STAT3 and log-cytokine was visualized by the cross plot. All graphs were created in GraphPad Prism 8.0.1 (GraphPad, San Diego, CA, USA). Findings with a p value < 0.05 were considered statistically significant.

Results

Immunobiochemical profile of clear cell renal cell carcinoma and healthy adjacent kidney tissue

Multiplex analysis has revealed that the tumor-derived tissue (tumor) has a distinct immunobiochemical profile compared to its healthy counterpart (normal). We have observed significant differences between the samples in 10 of 27 measured cytokines. The greatest differences were detected in the levels of G-CSF [two-tail *p*/Cohen's D: 0.0063/-0.829], IL-6 [two-tail *p*/Cohen's D: 0.039/−0.587], CXCL10 [two-tail *p*/Cohen's D: 0.00028/−1.405], CCL3 [two-tail *p*/Cohen's D: 0.00068/−1.461], and CCL4 [two-tail *p*/Cohen's D: <0.0001/−1.55] (Fig. 1, Table 2). These cytokines reached higher levels in the tumor than in the healthy tissue. The

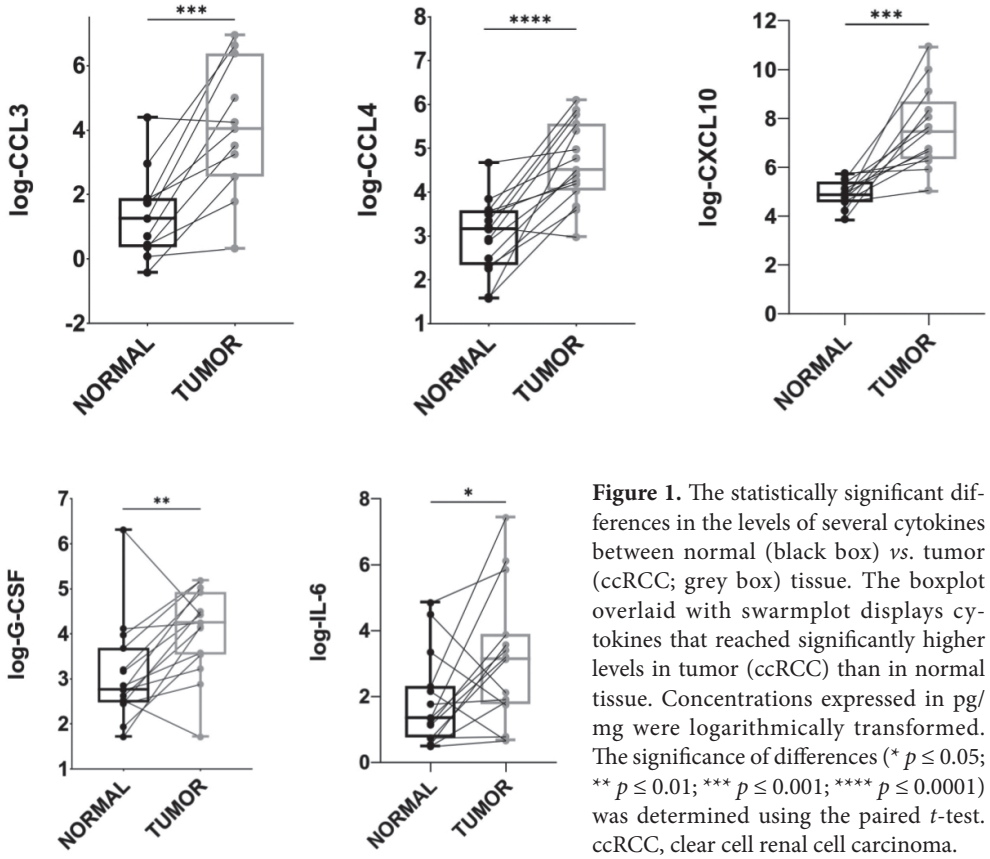

Figure 1. The statistically significant differences in the levels of several cytokines between normal (black box) *vs*. tumor (ccRCC; grey box) tissue. The boxplot overlaid with swarmplot displays cytokines that reached significantly higher levels in tumor (ccRCC) than in normal tissue. Concentrations expressed in pg/mg were logarithmically transformed. The significance of differences (* $p \leq 0.05$; ** $p \leq 0.01$; *** $p \leq 0.001$; **** $p \leq 0.0001$) was determined using the paired *t*-test. ccRCC, clear cell renal cell carcinoma.

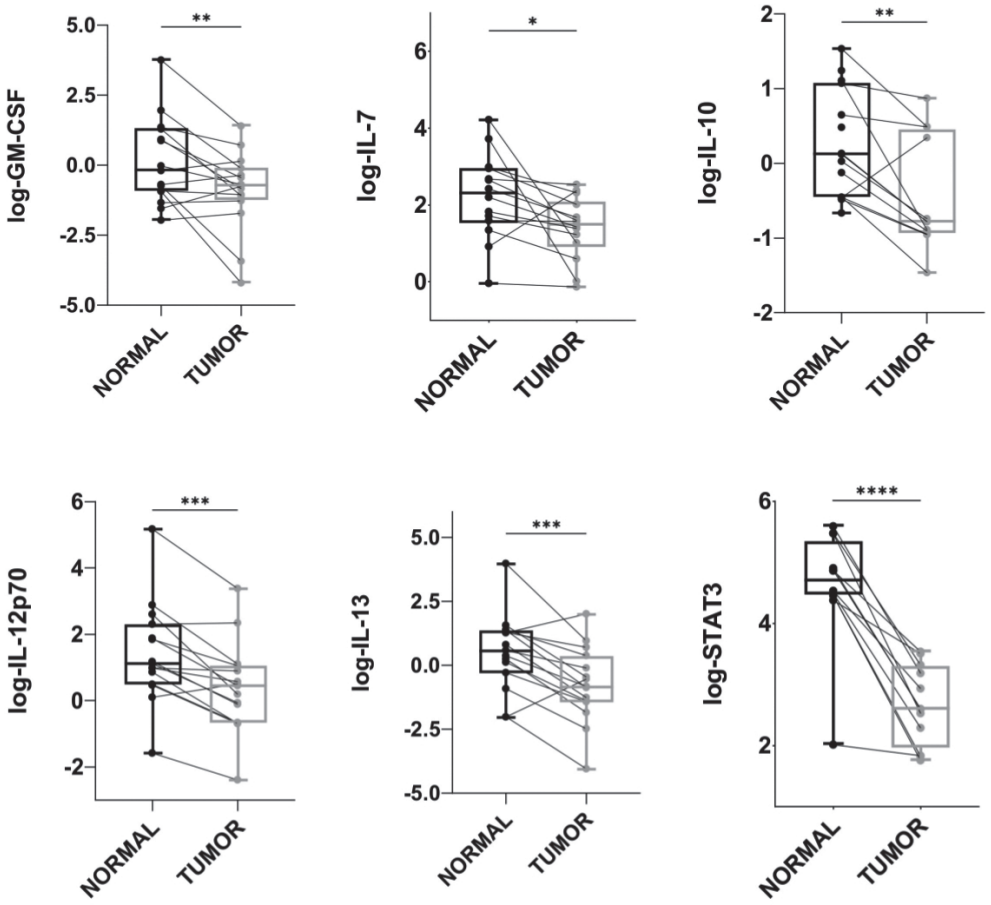

Figure 2. The statistically significant differences in the levels of several examined molecules between normal (black box) *vs*. tumor (ccRCC; grey box) tissue. The boxplot overlaid with swarmplot displays cytokines and STAT3 that reached significantly higher levels in normal than in tumor tissue (ccRCC). Concentrations expressed in pg/mg were logarithmically transformed. The significance of differences (* $p \leq 0.05$; ** $p \leq 0.01$; *** $p \leq 0.001$; **** $p \leq 0.0001$) was determined using the paired t-test. ccRCC, clear cell renal cell carcinoma.

amounts of the other five cytokines: GM-CSF [two-tail p/Cohen's D: 0.0086/0.788], IL-7 [two-tail p/Cohen's D: 0.036/0.599], IL-10 [two-tail *p*/Cohen's D: 0.0055/0.994], IL-12p70 [two-tail p/Cohen's D: 0.00013/1.343], and IL-13 [two-tail *p*/Cohen's D: 0.00092/1.079] were higher in kidney samples (Fig. 2, Table 2). Furthermore, STAT3 content was significantly lower in tumor than in normal tissue [two-tail *p*/Cohen's D: <0.0001/2.403]. The retrospective (*post hoc*) statistical power of the majority (all except GM-CSF and IL-6) of observed differences was shown to exceed 80% (Table 2). The heat map in Figure 3 provides a comprehensive view of the amounts of all examined molecules (27 cytokines and STAT3) in both types of tissue. It indicates that tumor tissue is more abundant in CCL2, IL-6, CXCL10, CCL3, G-CSF, and CCL4, while the other cytokines, including STAT3, appear to be present in on average higher concentrations in normal kidney tissue.

Correlation between cytokine and STAT3 tissue levels

To determine which of the measured cytokines may potentially activate STAT3, we have also analyzed the relationship between each of the measured cytokines and STAT3 in ccRCC and healthy kidney tissue distinctively using a linear regression model. A weak positive correlation with STAT3 was observed in ccRCC tissue for interleukins 2, 7, 10, 17A and CXCL10 [*p*/Adjusted R-Squared (Adj.R2): 0.002/0.16, 0.018/0.23, 0.001/0.28, 0.02/0.1, 0.016/0.4, respectively] (Fig. 4A–C, F, G). In healthy kidney tissue, CCL2 and CCL3 have shown a weak negative correlation with STAT3 levels [*p*/Adj.R2: 0.022/0.19 and 0.047/0.05, respectively], while PDGF-BB has shown a weak positive correlation with the amount of STAT3 [*p*/Adj.R2: 0.027/0.22] (Fig. 5). The strongest relationship has been observed for intratumoral STAT3 and two interleukins, IL-12p70 and IL-15 [*p*/Adj.R2: 0/0.82

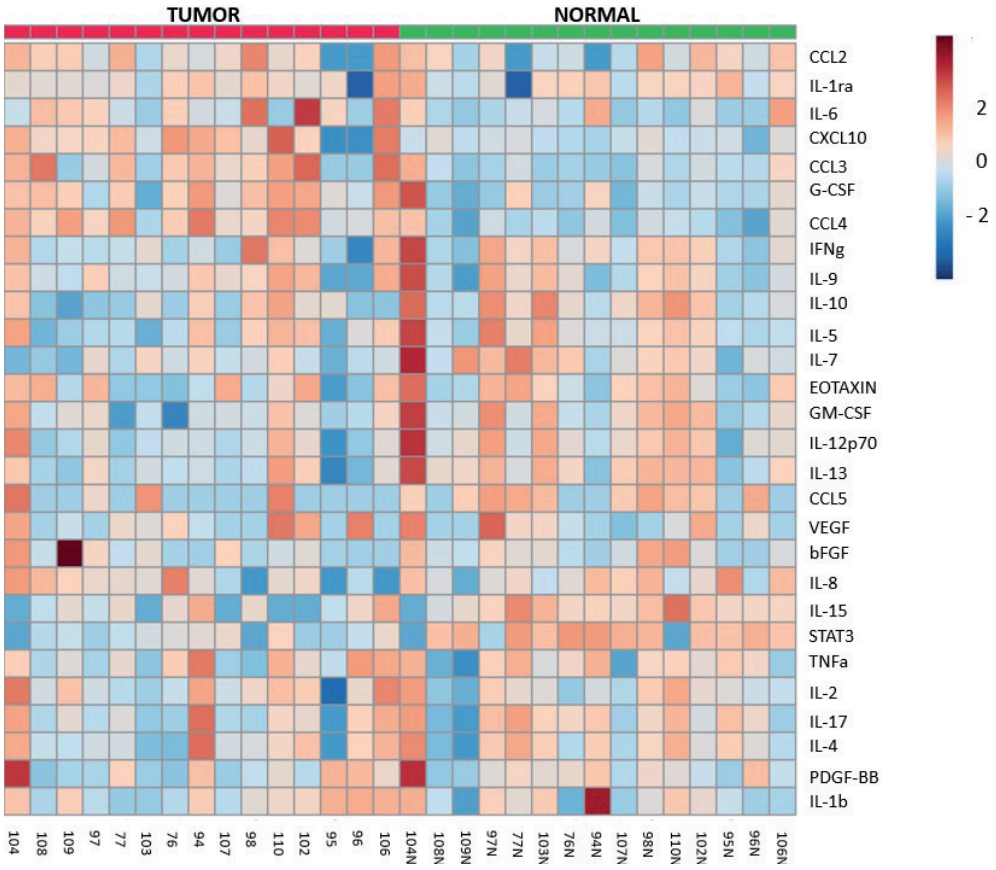

Figure 3. Tissue amounts of all examined molecules (27 cytokines and STAT3) in tissue samples from 15 patients. The heatmap includes data without gross outliers. Each row represents log-transformed concentrations (originally expressed in pg/mg) of a particular molecule (listed on the right side) in either tumor (ccRCC; cells overheaded by red boxes) or normal kidney tissue (cells overheaded by green boxes) and each column represents an individual sample. The intensity of the color is directly proportional to the log-concentration (orange >1; blue <1). The lower headings show the sample IDs. ccRCC, clear cell renal cell carcinoma.

Table 2. Comparison of statistically significant cytokine levels in normal and tumor (ccRCC) tissue

Target molecule	Normal tissue	Tumor tissue	Number of pairs (wo)	Differences	Statistic (*t*)	*p* value	Effect size	Statistical power (%)
G-CSF	3.1 ± 1.11	4.07 ± 0.96	15	0.973 ± 1.173	3.21	0.006**	0.830	84.72
GM-CSF	0.12 ± 1.55	0.92 ± 1.42	15	1.033 ± 1.310	3.05	0.009**	0.790	81.04
IL-6	1.79 ± 1.41	3.08 ± 2.06	15	1.293 ± 2.204	2.27	0.039*	0.590	56.16
IL-7	2.46 ± 1.4	1.7 ± 1.41	15	0.755 ± 1.260	2.32	0.036*	0.600	57.88
IL-10	0.25 ± 0.72	0.44 ± 0.76	12	0.662 ± 0.665	3.44	0.006**	0.990	94.70
IL-12p70	1.42 ± 1.52	0.39 ± 1.35	15	1.026 ± 0.764	5.20	<0.001***	1.340	99.79
IL-13	0.52 ± 1.5	0.75 ± 1.48	15	1.262 ± 1.169	4.18	<0.001***	1.080	97.26
CXCL10	4.74 ± 0.89	7.59 ± 1.68	13	2.677 ± 1.906	5.07	<0.001***	1.400	99.90
CCL3	1.19 ± 1.31	4.07 ± 1.99	11	2.684 ± 1.837	4.85	<0.001***	1.460	99.95
CCL4	2.99 ± 0.84	4.67 ± 0.93	15	1.676 ± 1.081	6.00	<0.0001****	1.550	99.98
STAT3	4.63 ± 0.89	2.75 ± 0.71	12	1.965 ± 0.818	8.32	<0.0001****	2.400	100.00

Data are mean ± SD. Two-tail *p* values (* $p \leq 0.05$, ** $p \leq 0.01$, *** $p \leq 0.001$, **** $p \leq 0.0001$) were calculated using the paired *t*-test and effect size was quantified by Cohen's D with magnitude: 0.2–0.6: trivial; 0.6–1.2: moderate; 1.2–2.0: large; >2.0: very large. The data (originally expressed in pg/mg) used in the analyses were logarithmically transformed. ccRCC, clear cell renal cell carcinoma; Differences, mean ± SD of differences in the levels of target molecules between each set of analyzed pairs of samples; SD, standard deviation; Statistical power = [1−β (probability of a type II error)]; wo, without outliers.

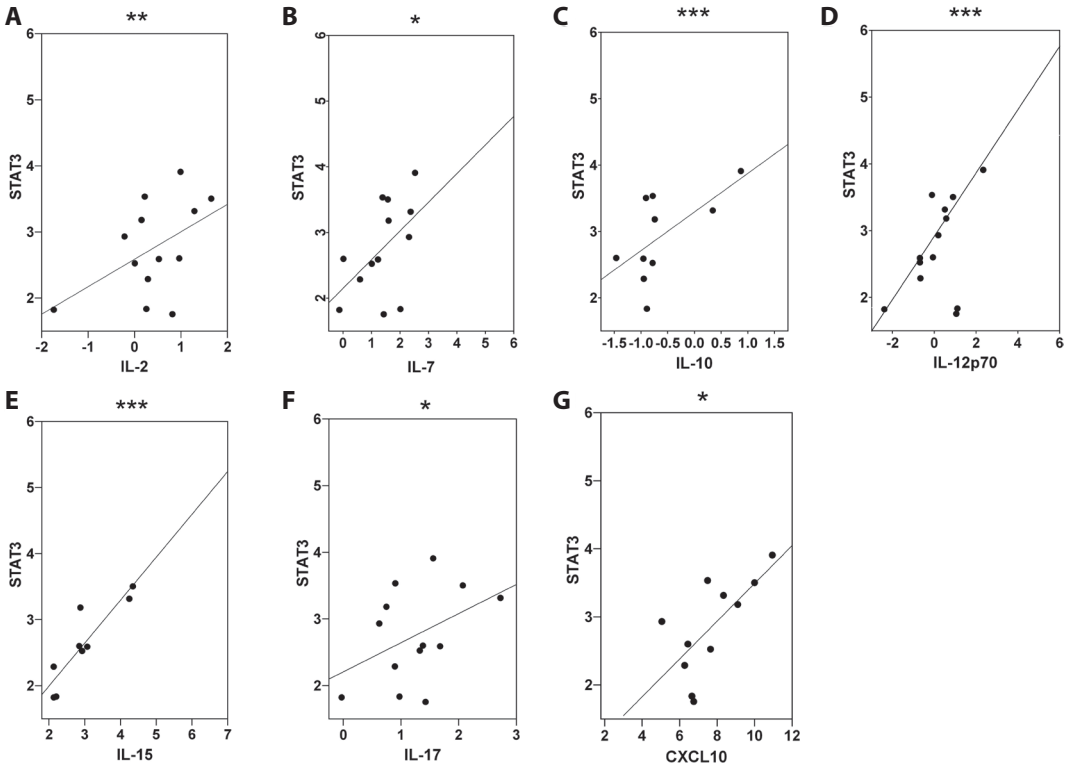

Figure 4. The statistically significant relationship between the levels of several cytokines (interleukins 2, 7, 10, 12p70, 15, 17 and chemokine CXCL10) and STAT3 in tumor tissue (ccRCC). **D, E.** Crossplots show a strong positive correlation. **A–C,, F, G.** Crossplots display weak positive correlation between the examined molecules. The significance of the relationship (* $p \leq 0.05$; ** $p \leq 0.01$; *** $p \leq 0.001$) was obtained using linear regression model. The concentrations of molecules used in the model were logarithmically transformed. ccRCC, clear cell renal cell carcinoma.

and 0/0.84, respectively] (Fig. 4D, E). The levels of these cytokines were positively correlated with STAT3. Table 3 represents a summary of the most significant molecules and their relationship with STAT3.

Changes in cytokine and STAT3 levels in relation to clinico-pathological characteristics

Finally, we have analyzed whether there are significant changes in the levels of individual cytokines and STAT3 in different clinical (TNM) and histopathological (NG) disease stages. According to our results, the levels of IL-1β and PDGF-BB levels have increased significantly with increasing NG [$p = 0.001$ and 0.025, respectively] (Fig. 6A,B; Table 4). Although no significant differences in IL-1β contents has been detected between tumors of NG2 and NG3 [adjusted p value ($p$adj) 0.213], with further progression of the disease (NG3 to NG4), IL-1β has increased significantly [$p$adj 0.034] (Fig. 6A, Table 4). The estimated difference was 0.74 pg/mg. When comparing the contents of IL-1β in NG2 tumors with NG4 tumors, the estimated difference was even

Table 3. Correlation between cytokine and STAT3 levels in normal and tumor (ccRCC) tissue

	Cytokine	p/AdjR2	
		Normal tissue	Tumor tissue
STAT3 *vs.*	IL-2	ns (0.552/−0.07)	0.002**/0.16
	IL-7	ns (0.149/0.05)	0.018*/0.23
	IL-10	ns (0.406/−0.06)	0.001***/0.28
	IL-12p70	ns (0.684/−0.07)	0***/0.82
	IL-15	ns (0.174/0)	0***/0.84
	IL-17	ns (0.198/0.06)	0.02*/0.1
	CXCL10	ns (0.194/0.05)	0.016*/0.4
	CCL2	0.22*/0.19	ns (0.943/−0.11)
	CCL3	0.047*/0.05	ns (0.842/−0.12)
	PDGF-BB	0.027*/0.22	ns (0.978/−0.09)

Linear regression model was used to determine two-tail p values (* $p \leq 0.05$; ** $p \leq 0.01$; *** $p \leq 0.001$) and adjusted R-squared (p/AdjR2). The data (originally expressed in pg/mg) used in the analysis were logarithmically transformed. STAT3, signal transducer and activator of transcription 3; ccRCC, clear cell renal cell carcinoma; ns, not significant.

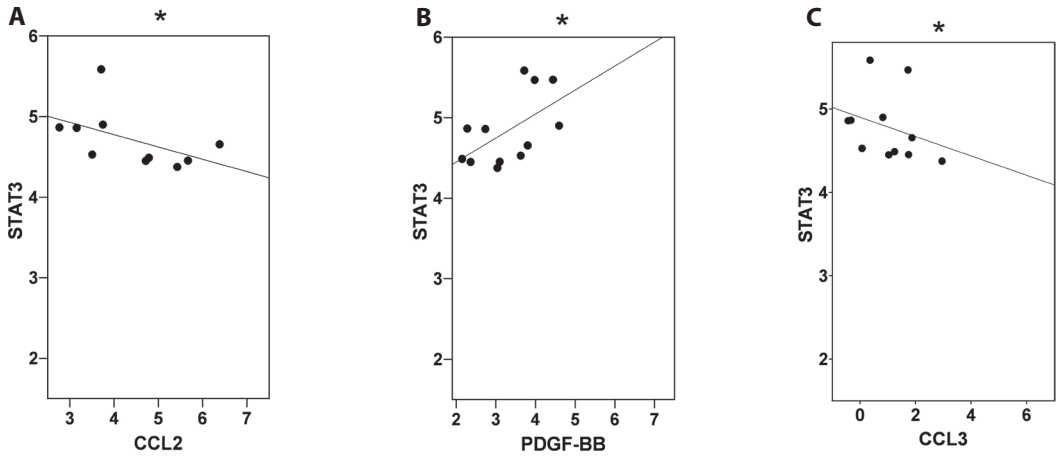

Figure 5. The statistically significant relationship between the levels of several cytokines (chemokines CCL2, CCL3 and growth factor PDGF-BB) and STAT3 in macroscopically healthy (normal) kidney tissue. **A, C.** Crossplots show weak negative correlation. **B.** Crossplot displays weak positive correlation. The significance of the relationship (* $p \leq 0.05$) was obtained using linear regression model. The concentrations of molecules used in the model were logarithmically transformed.

greater [1.13 pg/mg; *p*adj 0.003]. Regarding intratumoral PDGF-BB, the elevation across NGs was rather gradual, and the differences between NG2 *vs*. NG3 and NG3 *vs*. NG4 were not significant [*p*adj 0.792 and 0.089, respectively] (Fig. 6B, Table 4). However, a *post hoc* Tukey test has revealed that the tumor contents of PDGF-BB in NG4 tumors were significantly higher (by 1.7 pg/mg) than in NG2 specimens [*p*adj 0.04]. Furthermore, tumor progression from NG2 to

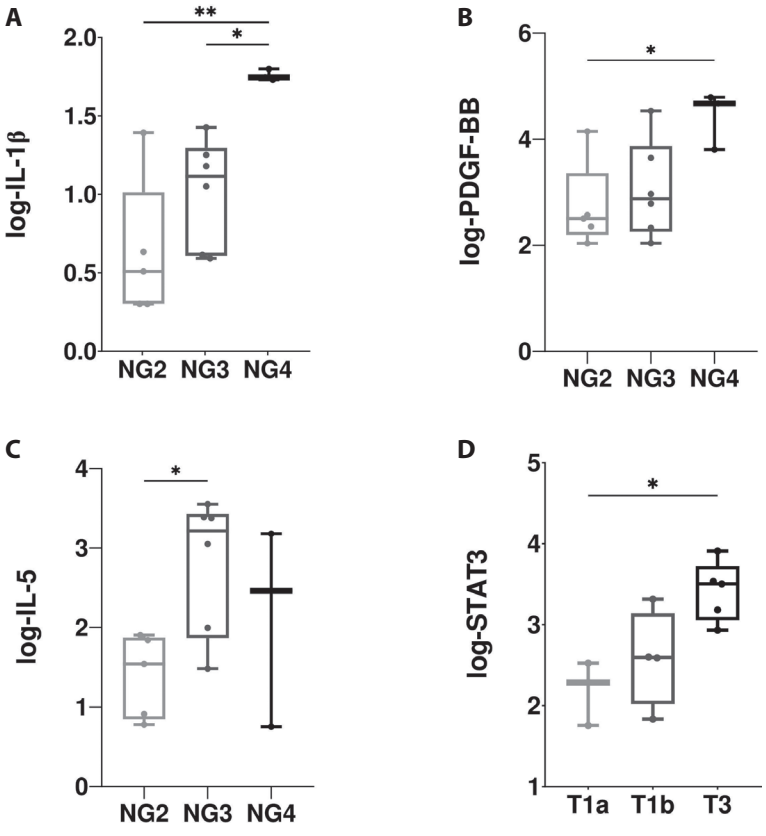

Figure 6. Changes in intratumoral levels of several cytokines and STAT3 in different histopathological (NG2, NG3, NG4; **A–C**) and clinical (T1a, T1b, T3; **D**) stages of ccRCC. The significance of the changes (* $p \leq 0.05$; ** $p \leq 0.01$) was calculated using the Welch ANOVA test followed by Tukey's HSD pairwise comparison. The concentrations of the molecules used in the tests were logarithmically transformed. ccRCC, clear cell renal cell carcinoma; NG, nuclear grading; STAT3, signal transducer and activator of transcription 3; T1a, tumor confined to kidney (<4 cm); T1b, tumor confined to kidney (>4 cm, but <7 cm); T3, tumor extends into major veins or perinephric tissues but not into ipsilateral adrenal gland or beyond Gerota's fascia; Tukey's HSD, Tukey's honestly significant difference.

NG3 was also accompanied by a significant increase in IL-5 levels [*p*adj 0.04; the estimated difference was 1.41 pg/mg] (Fig. 6C, Table 4). IL-5 levels have decreased with further progression of the disease (from NG3 to NG4), although this change was not significant [*p*adj 0.518].

From all the analyzed molecules, only STAT3 tumor tissue contents have displayed significant changes with increasing TNM stage [*p*adj 0.023] (Table 4). There has been a significant difference in intratumoral STAT3 levels between T1a and T3 tumors [*p*adj 0.015]. Tumors of the higher clinical stage (T3) had 1.22 pg/mg higher levels of STAT3 than T1 tumors (Fig. 6D, Table 4). Differences in STAT3 tissue expression between T1a *vs*. T1b and T1b *vs*. T3 were not significant (*p*adj 0.532 and 0.063, respectively). Unfortunately, T2 tumors could not be assessed as they were missing in our data set.

Discussion

Cytokines are well known for their ability to regulate immune system reactions. Many of them play a critical role in the initiation and progression of cancer (Kartikasari et al. 2021; Lan et al. 2021). In the present study, we observed significantly higher levels of G-CSF, IL-6, CXCL10, CCL3 and CCL4 in human ccRCC tissue than in healthy adjacent kidneys. This may indicate their potentially tumor-promoting character. Several other studies support this notion. For instance, Gudowska-Sawczuk et al. (2020) also reported increased levels of CXCL10 in RCC. In addition, others suggest that this chemokine may be a biomarker of tumor metastasis and an indicator of poor prognosis (Lasagni et al. 2003; Suyama et al. 2005; Utsumi et al. 2014; Wightman et al. 2015). However, contradictory results also exist. The antiangiogenic and antitumor properties of CXCL10 were demonstrated and this chemokine is supposed to be an indicator of a good prognosis (Arenberg et al. 1996; Sato et al. 2007; Jain et al. 2008; Aronica et al. 2009; Motoshima et al. 2016). Enhanced expression of CCL4 was confirmed in different types of human cancers, including ccRCC, where it even showed a significant correlation with an advanced stage of the disease (Erreni et al. 2009; Pitarresi et al. 2016; Li et al. 2018; Korbecki et al. 2020). Furthermore, we have detected significantly higher CXCL10 and CCL4 in ccRCC than in normal tissue in our previous work (Vargová et al. 2022).

Potentially tumor-promoting effects have also been observed for G-CSF in a substantial number of various solid tumor specimens (including RCC) (Gerharz et al. 2001; Liu et al. 2017, 2020). Intratumoral CCL3 also acts in favor of the tumor rather than the host. According to Najjar et al. (2017), it can attract polymorphonuclear myeloid-derived suppressor cells (PMN-MDSC) to the TME of RCC. On the other hand, a report on its ability to enhance antitumor immunity exists as well (Ntanasis-Stathopoulos et al. 2020). Regarding

Table 4. Changes in cytokines and STAT3 levels in tumor tissue (ccRCC) according to clinical (TNM) and histopathological (NG) disease stages of the disease

Target molecule	Analysis of variance test			Multiple comparisons test			
	Disease feature	*p* value	*F* (DFn; DFd)	Disease stages compared	Estimate (pg/mg)	95% CI	*p*adj.
IL-1β	NG	0.001**	25.84 (2; 6.1)	2–3	0.39	−0.19–0.98	0.213 ns
				2–4	1.13	0.42–1.83	0.003**
				3–4	0.74	0.06–1.42	0.034*
IL-5	NG	0.069 ns	4.98 (2; 4.7)	2–3	1.41	0.03–2.8	0.046*
				2–4	0.74	−0.93–2.41	0.483 ns
				3–4	−0.68	−2.29–0.94	0.518 ns
PDGF-BB	NG	0.025*	6.69 (2; 6.73)	2–3	0.33	−1.02–1.67	0.792 ns
				2–4	1.70	0.08–3.32	0.040*
				3–4	1.37	−0.2–2.95	0.089 ns
STAT3	TNM	0.023*	8.94 (2; 4.98)	T1a–T1b	0.40	−0.6–1.4	0.532 ns
				T1a–T3	1.22	0.27–2.18	0.015*
				T1b–T3	0.83	−0.05–1.70	0.063 ns

p values (* $p \leq 0.05$; ** $p \leq 0.01$) were obtained using the Welch ANOVA test. *Post-hoc* Tukey test was used to compare the means of cytokine levels between different disease stages. The data (originally expressed in pg/mg) used in the analyses were logarithmically transformed. ccRCC, clear cell renal cell carcinoma; CI, confidence interval; DFn, degrees of freedom numerator; DFd, degrees of freedom denomitaor; *F*, a distribution of the ratio of two estimates of variance (variance between groups and within groups); NG, nuclear grade; ns, not significant; *p*adj., adjusted *p* value; TNM, tumor node metastasis staging system; T1a, tumor confined to kidney (<4 cm); T1b, tumor confined to kidney (>4 cm, but <7 cm); T3, tumor extends into major veins or perinephric tissues but not into ipsilateral adrenal gland or beyond Gerota's fascia.

IL-6, this interleukin is well known to significantly support almost all cancer features (Chonov et al. 2019). In accordance with our results, several other authors detected increased levels of IL-6 in either serum or tumor tissue from patients with RCC (Takenawa et al. 1991; Karczewska Aldona and Mackiewicz 2001; Negrier et al. 2004; Polimeno et al. 2013).

Regarding healthy kidney tissue, we have observed significantly higher concentrations of GM-CSF, IL-7, IL-10, IL-12p70, and IL-13 than in their tumor counterparts. We suppose that this may reflect the activation of host defense mechanisms as a response to the nearby tumor and indicate their antitumor properties. However, the data available on these cytokines is rather ambiguous. In general, most interleukins tend to exert both anti- and pro-tumor activities (Lissoni et al. 2020). For example, IL-7 and IL-10 can both enhance the activity of cytotoxic $CD8^+$ lymphocytes (Oft 2014; Lin et al. 2017), but high levels of IL-7 in tumor tissue can indicate a poor prognosis (Liu et al. 2014; Barata et al. 2019), and IL-10 can down-regulate antigen presentation and thus diminish antitumor immunity (Oft 2014). According to other studies, the character of IL-12 and IL-13 is somewhat more one-sided. IL-12 enhances the activity of cytotoxic cells and inhibits the effects of immunosuppressive cells (Zhao et al. 2012; Tugues et al. 2015). Our assumption of its antitumor character is further supported by several preclinical studies on a variety of human cancers (Nguyen et al. 2020). On the other hand, IL-13 appears to have rather tumor-promoting effects. It has been detected in several solid tumors (breast, oral squamous cell, and colorectal carcinoma), including ccRCC (Aziz et al. 2010; Srabovic et al. 2011; Formentini et al. 2012; Chang et al. 2015). Furthermore, it may promote metastasis and favor M2-macrophage polarization, and its high tissue levels in patients with localized ccRCC may indicate adverse outcomes (Sinha et al. 2005; Formentini et al. 2012; Chang et al. 2015). However, our results of increased levels of IL-13 in kidney tissue seem to conflict with these. Lastly, regarding GM-CSF, it has been shown to be produced by RCC cancer cells (Gerharz et al. 2001), which is also inconsistent with our findings. On the other hand, GM-CSF present in other types of cancer types (e.g., human colorectal cancer and melanoma) may indeed display antitumor activity (Urdinguio et al. 2013; Grotz et al. 2014).

To see whether the trend observed by our study is preserved also at the transcriptional level, we have compared our results with the data on gene expressions using the interactive online database GEPIA [http://gepia.cancer-pku.cn/, accessed on April 21, 2023] (Tang et al. 2017). Differential gene analysis performed on 523 ccRCC samples and 100 samples from normal renal cortex tissue shows that the expression of CXCL10, CCL3, and CCL4 is markedly up-regulated in the tumor (Table S1 in Supplementary materials). This agrees with our data. However, there are several discrepancies. According to GEPIA results, ccRCC also shows an increase in VEGF and CXCL11 expression, which we did not observe. On the other hand, the significant differences in G-CSF, GM-CSF, IL-6, IL-7, IL12, and IL-13 tissue levels detected by our study, were not confirmed by GEPIA (Table S1).

Next, we examined the dynamics of cytokines in tumor specimens according to their NG. Significant differences in the levels of the two cytokines were observed. The more aggressive NG4 tumors contained significantly higher amounts of IL-1β and PDGF-BB than the NG2 tumors. Therefore, we suppose IL-1β and PDGF-BB could represent promising therapeutic targets. In fact, both IL-1β and PDGF are well known to be involved in the development of malignant diseases. Increased IL-1β production within the TME is believed to promote tumor growth and metastasis through different mechanisms (Bent et al. 2018). PDGF signaling is often overactive in various malignancies, and several inhibitors of PDGFR have already been developed and used for cancer treatment (Heldin 2013). However, contradictory results exist. Lee et al. (2016) suggested that neither intratumoral nor serum levels of IL-1β are associated with the progression RCC, and IL-1β treatment can even inhibit malignant features of RCC cell lines. Another study has demonstrated that overexpression of PDGF-BB by human kidney cancer cells also significantly inhibits tumor growth and progression *in vivo* (Wang et al. 2015). According to our results, the progression of ccRCC from NG2 to NG3 and from NG3 to NG4 was further accompanied by a significant increase in intra-tumoral IL-5 and IL-1β levels, respectively. Interestingly, the IL-5 content in the NG4 samples was lower than in NG3. This difference was not significant, but may indicate the protective character of this interleukin, which disappears with tumor progression.

The discrepancies between the studies on cytokines mentioned above can be explained by the following: 1) Cytokines are very pleiotropic molecules, and they do not act alone; highly complex interactions among them exist (Elias and Zitnik 1992); 2) The TME of any solid neoplasia has a highly complex and continuously evolving structure consisting of noncellular compartments and diverse cellular populations (Anderson and Simon 2020). We believe that further and more detailed analyzes may give a more clear understanding of the complex nature of any of the cytokines presented and their role in the pathogenesis of ccRCC.

The next part of our study focused on STAT3 and its relationship with cytokines. It is well-known that the majority of cytokines exert their effects through the JAK/STAT pathway. This pathway has recently been extensively studied in association with tumorigenesis (Brooks and Putoczki 2020). Overstimulation of STAT3 in genitourinary tumors, including renal neoplasms, is associated with tumor progression and a poor patient prognosis (Horiguchi et al. 2002; Guo et al. 2009; Santoni et al. 2015). The reduced activity of STAT3 has, on the other hand, significant inhibitory effects on RCC

(Xin et al. 2009; Li et al. 2013; Shanmugam et al. 2015; Kim et al. 2016). On the contrary, the results of the present study are not in line with this generally accepted concept of the tumor-promoting character of STAT3. We have detected significantly higher STAT3 concentrations in normal tissue than in ccRCC specimens. This discrepancy may be attributed to the limitations of the detection method used. Since the tissue homogenates were (according to the protocol) centrifugated at 7170 rpm, we assume that the supernatant used in the ELISA probably contained only or mainly a cytoplasmic cell compartment. Therefore, it remains uncertain whether only inactive (unphosphorylated, U-STAT3) or both active (phosphorylated, p-STAT3) and inactive forms of STAT3 were detected. Nevertheless, Masuda et al. (2009) have also detected significantly lower absolute levels of STAT3 mRNA in RCC tissue compared with nontumor surgical samples. In contrast to these are the results of GEPIA. Although STAT3 transcriptional levels in tumors were slightly lower than in kidneys, the difference was negligible (Tang et al. 2017).

Intratumoral STAT3 in our samples did not show any significant relationship with NG. Masuda et al. (2009) reported similar results, but these authors also did not report any significant correlation between STAT3 and TNM. On the contrary, our findings have shown that STAT3 protein levels increased significantly with tumor progression from T1 to T3. As for the transcriptional level, the GEPIA results did not show any similar effect. STAT3 expression appears to be constant as the disease stage increases (Tang et al. 2017). Therefore, further analyzes are indispensable to validate the potential relationship between the dynamics of STAT3 tumor content and the progression of the disease.

Last but not least, two interleukins (IL-12p70 and IL-15) have shown a significant relationship with STAT3 levels in tumors. The correlation was positive, suggesting that there is some interaction between these cytokines and STAT3. However, assuming that STAT3 levels in our samples represent the inactive form, we can hypothesize that the correlation of these two cytokines with the active (nuclear) form of STAT3 would be negative. This would imply that they probably do not act as STAT3 activators in the tumor environment but may signal through different STATs, which is eventually demonstrated by other studies. For example, IL-15 in lymphocytes can activate both Jak3/STAT5 and Jak1/STAT3 pathways, while in mast cells it induces Tyk2/STAT6 (Mishra et al. 2014). Similarly, IL-12 in TH1 and NK cells is known to signal mainly through Jak2 and Tyk2, which leads to the phosphorylation of STAT4. Although STAT1, STAT3, and STAT5 can also be phosphorylated in response to IL-12 (Gollob et al. 1998; Hamza et al. 2010).

Our study has several limitations. First, the data set is limited and does not cover patients in the four stages of NG and TNM. However, these are only preliminary results, and statistical power indicates that our sample size is sufficient to detect significant differences. Second, we assume that macroscopically healthy renal tissue may have been affected to some extent by systemic changes in the patient's immune system. Thus, it would be worth comparing the cytokine profiles of ccRCC tissue with kidney specimens of subjects without renal malignancy or other diseases. Next, it would be advisable to perform a detailed cellular analysis of ccRCC TME, as it could help us better understand the complex immunobiochemical mechanisms of this cancer. Last but not least, measurement of the total and tyrosine 705 (Y705) phosphorylated forms of STAT3 separately is necessary to elucidate its role in the pathogenesis of ccRCC more deeply.

Conclusion

The present study has confirmed the pathological relevance of G-CSF, IL-6, CXCL10, CCL3 and CCL4 in the development of ccRCC, but their specific roles in the pathogenesis of this cancer need to be further elucidated. Second, our results suggest that progression to a more aggressive tumor phenotype is associated with an increase in IL-1β and PDGF-BB. Therefore, these cytokines appear to be most clinically relevant and could probably be used in the development of new therapeutic methods. Next, we detected significantly lower levels of STAT3 in tumors than in normal tissue. Patients with T3 had significantly higher intratumoral STAT3 content than patients with T1, which may indicate STAT3 as a marker of disease progression. Lastly, a significant correlation was detected between intratumoral STAT3 and two interleukins (IL-12p70 and IL-15). However, further analysis is warranted to explain the intricate mechanisms behind cytokine and STAT3 signaling in ccRCC.

Author contributions. Conceptualization, DV and MŠ; methodology, DV, MD, JD, and LB; software, MG; validation and formal analysis, DV, MD, resources, JD, LB, and JĽ; data curation, MG; writing – original draft preparation, DV; writing – review and editing, MŠ, SF; visualization, DV; supervision, MŠ; project administration, DV; funding acquisition, MŠ, SF, and JŠ. All authors have read and agreed to the published version of the manuscript.

Funding. This publication has been produced with the support of grants VEGA 1/0428/21, VEGA 1/0072/23, APVV-19-0033, and the integrated operational program infrastructure for the project New Possibilities for the Management of Serious Diseases in Medical and Preventive Care with Regard to the Safety of Health Professionals, ITMS: 313011AUA5, co-financed by the European Regional Development Fund.

Institutional ethics committee statement. This study was carried out in accordance with the Declaration of Helsinki and approved by the Institutional Ethics Committee of the Jessenius Faculty of Medicine of Martin Comenius University in Bratislava (protocol code No. 19/2019, date of approval). The collection and handling

of biological material were in accordance with Slovakian and European legislation.

Informed consent statement. Each participant was presented with the key elements of the study and voluntarily signed the informed consent. Written informed consent has been obtained from all subjects involved in the study.

Acknowledgments. Technical support by Katarína Jesenská.

Conflicts of interest. The authors declare that they have no conflict of interest. The sponsors had no role in the design of the study; in the collection, analysis or interpretation of data, in the writing of the manuscript, or in the decision to publish the results.

References

Anderson NM, Simon MC (2020): The tumor microenvironment. Curr. Biol. **30,** R921-R925 https://doi.org/10.1016/j.cub.2020.06.081

Arenberg DA, Kunkel SL, Polverini PJ, Morris SB, Burdick MD, Glass MC, Taub DT, Iannettoni MD, Whyte RI, Strieter RM (1996): Interferon-gamma-inducible protein 10 (IP-10) is an angiostatic factor that inhibits human non-small cell lung cancer (NSCLC) tumorigenesis and spontaneous metastases. J. Exp. Med. **184,** 981-992 https://doi.org/10.1084/jem.184.3.981

Aronica SM, Raiber L, Hanzly M, Kisela C (2009): Antitumor/antiestrogenic effect of the chemokine interferon inducible protein 10 (IP-10) involves suppression of VEGF expression in mammary tissue. J. Interferon Cytokine Res. **29,** 83-92 https://doi.org/10.1089/jir.2008.0034

Aziz MH, Hafeez BB, Sand JM, Pierce DB, Aziz SW, Dreckschmidt NE, Verma AK (2010): Protein kinase Cε mediates Stat3Ser727 phosphorylation, Stat3-regulated gene expression, and cell invasion in various human cancer cell lines through integration with MAPK cascade (RAF-1, MEK1/2, and ERK1/2). Oncogene **29,** 3100-3109 https://doi.org/10.1038/onc.2010.63

Barata JT, Durum SK, Seddon B (2019): Flip the coin: IL-7 and IL-7R in health and disease. Nat. Immunol. **20,** 1584-1593 https://doi.org/10.1038/s41590-019-0479-x

Bautista JPA (2019): The Role of STAT3 Phosphorylation State in Clear Cell Renal Cell Carcinoma (ccRCC) (Dissertation thesis). The Autonomous University of Barcelona

Bent R, Moll L, Grabbe S, Bros M (2018): Interleukin-1 beta – a friend or foe in malignancies? Int. J. Mol. Sci. **19,** 2155 https://doi.org/10.3390/ijms19082155

Brooks AJ, Putoczki T (2020): JAK-STAT signalling pathway in cancer. Cancers **12,** 1971 https://doi.org/10.3390/cancers12071971

Cairns P (2011): Renal cell carcinoma. Cancer Biomarkers **9,** 461-473 https://doi.org/10.3233/CBM-2011-0176

Chang Y, Xu L, An H, Fu Q, Chen L, Lin Z, Xu J (2015): Expression of IL-4 and IL-13 predicts recurrence and survival in localized clear-cell renal cell carcinoma. Int. J. Clin. Exp. Pathol. **8,** 1594-1603

Chonov DC, Ignatova MMK, Ananiev JR, Gulubova MV (2019): IL-6 activities in the tumour microenvironment. Part 1. Open Access Maced. J. Med. Sci. **7,** 2391-2398 https://doi.org/10.3889/oamjms.2019.589

di Pietro G, Luu HN, Spiess PE, Sexton W, Dickinson S, Parker A, Park JY (2018): Biomarkers and new therapeutic targets in renal cell carcinoma. Eur. Rev. Med. Pharmacol. Sci. **22,** 5874-5891

Elias JA, Zitnik RJ (1992): Cytokine-cytokine interactions in the context of cytokine networking. Am. J. Resp. Cell Mol. Biol. **7,** 365-367 https://doi.org/10.1165/ajrcmb/7.4.365

Erreni M, Bianchi P, Laghi L, Mirolo M, Fabbri M, Locati M, Mantovani A, Allavena P (2009): Expression of chemokines and chemokine receptors in human colon cancer. Methods Enzymol. **460,** 105-121 https://doi.org/10.1016/S0076-6879(09)05205-7

Faul F, Erdfelder E, Buchner A, Lang AG (2009): Statistical power analyses using G*Power 3.1: Tests for correlation and regression analyses. Behav. Res. Methods **41,** 1149-1160 https://doi.org/10.3758/BRM.41.4.1149

Formentini A, Braun P, Fricke H, Link KH, Henne-Bruns D, Kornmann M (2012): Expression of interleukin-4 and interleukin-13 and their receptors in colorectal cancer. Int. J. Colorectal Dis. **27,** 1369-1376 https://doi.org/10.1007/s00384-012-1456-0

Fox JWS (2019): An R Companion to Applied Regression (3rd Edition). Thousand Oaks CA: Sage

Garfield KLC (2021): Renal Cell Cancer. Treasure Island (FL), StatPearls Publishing

Gerharz CD, Reinecke P, Schneider EM, Schmitz M, Gabbert HE (2001): Secretion of GM-CSF and M-CSF by human renal cell carcinomas of different histologic types. Urology **58,** 821-827 https://doi.org/10.1016/S0090-4295(01)01371-1

Gollob JA, Murphy EA, Mahajan S, Schnipper CP, Ritz J, Frank DA (1998): Altered interleukin-12 responsiveness in Th1 and Th2 cells is associated with the differential activation of STAT5 and STAT1. Blood **91,** 1341-1354 https://doi.org/10.1182/blood.V91.4.1341

Grotz TE, Kottschade L, Pavey ES, Markovic SN, Jakub JW (2014): Adjuvant GM-CSF improves survival in high-risk stage IIIC melanoma. Am. J. Clin. Oncol. **37,** 467-472 https://doi.org/10.1097/COC.0b013e31827def82

Gudowska-Sawczuk M, Kudelski J, Mroczko B (2020): The role of chemokine receptor CXCR3 and its ligands in renal cell carcinoma. Int. J. Mol. Sci. **21,** 8582 https://doi.org/10.3390/ijms21228582

Guo C, Yang G, Khun K, Kong X, Levy D, Lee P, Melamed J (2009): Activation of Stat3 in renal tumors. Am. J. Transl. Res. **1,** 283-290

Hamza T, Barnett JB, Li B (2010): Interleukin 12 a key immunoregulatory cytokine in infection applications. Int. J. Mol. Sci. **11,** 789-806 https://doi.org/10.3390/ijms11030789

Heidegger I, Pircher A, Pichler R (2019): Targeting the tumor microenvironment in renal cell cancer biology and therapy. Front. Oncol. **9,** 490 https://doi.org/10.3389/fonc.2019.00490

Heldin CH (2013): Targeting the PDGF signaling pathway in tumor treatment. Cell Commun. Signal. **11,** 97 https://doi.org/10.1186/1478-811X-11-97

Hirano T, Ishihara K, Hibi M (2000): Roles of STAT3 in mediating the cell growth, differentiation and survival signals relayed through the IL-6 family of cytokine receptors. Oncogene **19,** 2548-2556 https://doi.org/10.1038/sj.onc.1203551

Horiguchi A, Oya M, Shimada T, Uchida A, Marumo K, Murai M (2002): Activation of signal transducer and activator of transcription 3 in renal cell carcinoma: a study of incidence and its association with pathological features and clinical outcome. J. Urol. **168,** 762-765 https://doi.org/10.1016/S0022-5347(05)64741-6

Jain V, Armah HB, Tongren JE, Ned RM, Wilson NO, Crawford S, Joel PK, Singh MP, Nagpal AC, Dash A, et al. (2008): Plasma IP-10, apoptotic and angiogenic factors associated with fatal cerebral malaria in India. Malar. J. **7,** 83 https://doi.org/10.1186/1475-2875-7-83

Kang M, Choi J, Kim J, Sung HH, Jeon HG, Jeong BC, Jeon SS, Lee HM, Park SH, Song C, et al. (2020): Prognostic impact of bone metastasis on survival outcomes in patients with metastatic renal cell carcinoma treated by first line tyrosine kinase inhibitors: A propensity-score matching analysis. J. Cancer **11,** 7202-7208 https://doi.org/10.7150/jca.48062

Karczewska A, Mackiewicz A, Mackiewicz-Wysocka M, Kwias Z (2001): Expression of interleukin-6 and its receptor subunits in the microenviroment of renal cell cancer. Współ. Onkol. **5,** 45-47 (in Polish)

Kartikasari AER, Huertas CS, Mitchell A, Plebanski M (2021): Tumor-induced inflammatory cytokines and the emerging diagnostic devices for cancer detection and prognosis. Front. Oncol. **11,** 692142 https://doi.org/10.3389/fonc.2021.692142

Kassambara A (2020): ggpubr: ‚ggplot2' Based Publication Ready Plots. R Package Version 0.4.0.999 https://rpkgs.datanovia.com/ggpubr/

Kassambara A (2021): rstatix: Pipe-Friendly Framework for Basic Statistical Tests. R Package Version 0.7.0 https://CRAN.R-project.org/package=rstatix

Kim C, Baek SH, Um JY, Shim BS, Ahn KS (2016): Resveratrol attenuates constitutive STAT3 and STAT5 activation through induction of PTPε and SHP-2 tyrosine phosphatases and potentiates sorafenib-induced apoptosis in renal cell carcinoma. BMC Nephrology **17,** 19 https://doi.org/10.1186/s12882-016-0233-7

Korbecki J, Grochans S, Gutowska I, Barczak K, Baranowska-Bosiacka I (2020): CC chemokines in a tumor: A review of pro-cancer and anti-cancer properties of receptors CCR5, CCR6, CCR7, CCR8, CCR9, and CCR10 ligands. Int. J. Mol. Sci. **21,** 7619 https://doi.org/10.3390/ijms21207619

Lan T, Chen L, Wei X (2021): Inflammatory cytokines in cancer: Comprehensive understanding and clinical progress in gene therapy. Cells **10,** 100 https://doi.org/10.3390/cells10010100

Lasagni L, Francalanci M, Annunziato F, Lazzeri E, Giannini S, Cosmi L, Sagrinati C, Mazzinghi B, Orlando C, Maggi E, et al. (2003): An alternatively spliced variant of CXCR3 mediates the inhibition of endothelial cell growth induced by IP-10, Mig, and I-TAC, and acts as functional receptor for platelet factor 4. J. Exp. Med. **197,** 1537-1549 https://doi.org/10.1084/jem.20021897

Lee CH, Sun CY, Lu SC, Li CH, Yang JR, Hsieh WY (2016): IL-1b mediates anti-progression activities in renal cell carcinoma by inducing MCP-1. Ann. Oncol. (Suppl. 8) **27,** VIII11 https://doi.org/10.1093/annonc/mdw525.35

Lee H, Jeong AJ, Ye SK (2019): Highlighted STAT3 as a potential drug target for cancer therapy. BMB Rep. **52,** 415-423 https://doi.org/10.5483/BMBRep.2019.52.7.152

Li L, Liu YD, Zhan YT, Zhu YH, Li Y, Xie D, Guan XY (2018): High levels of CCL2 or CCL4 in the tumor microenvironment predict unfavorable survival in lung adenocarcinoma. Thorac Cancer **9,** 775-784 https://doi.org/10.1111/1759-7714.12643

Lin J, Zhu Z, Xiao H, Wakefield MR, Ding VA, Bai Q, Fang Y (2017): The role of IL-7 in immunity and cancer. Anticancer Res. **37,** 963-968 https://doi.org/10.21873/anticanres.11405

Li S, Priceman SJ, Xin H, Zhang W, Deng J, Liu Y, Huang J, Zhu W, Chen M, Hu W, et al. (2013): Icaritin Inhibits JAK/STAT3 signaling and growth of renal cell carcinoma. PLoS One **8,** e81657 https://doi.org/10.1371/journal.pone.0081657

Lissoni P, Messina G, Pelizzoni F, Rovelli F, Brivio F, Monzon A, Crivelli N, Lissoni A, Tassoni S, Sassola A, et al. (2020): The fascination of cytokine immunological science. J. Infectiology **3,** 18-28 https://doi.org/10.29245/2689-9981/2020/1.1155

Liu L, Liu Y, Yan X, Zhou C, Xiong X (2020): The role of granulocyte colony stimulating factor in breast cancer development: A review. Mol. Med. Rep. **21,** 2019-2029 https://doi.org/10.3892/mmr.2020.11017

Liu ZH, Wang MH, Ren HJ, Qu W, Sun LM, Zhang QF, Qiu XS, Wang EH (2014): Interleukin 7 signaling prevents apoptosis by regulating bcl-2 and bax via the p53 pathway in human non-small cell lung cancer cells. Int. J. Clin. Exp. Pathol. **7,** 870-881

Liu Z, Zhu Y, Wang Y, Fu Q, Fu H, Wang Z, Zhang J, Li G, Xu J, Dai B (2017): Prognostic value of granulocyte colony-stimulating factor in patients with non-metastatic clear cell renal cell carcinoma. Oncotarget **8,** 69961-69971 https://doi.org/10.18632/oncotarget.19540

Maechler M, Rousseeuw P, Croux C, Todorov V, Ruckstuhl A, Salibian-Barrera M, Verbeke T, Koller M, Conceicao E, di Palma MA (2021): Robustbase: Basic Robust Statistics R Package Version 0.93-7 http://CRAN.R-project.org/package=robustbase

Masuda A, Kamai T, Abe H, Arai K, Yoshida KI (2009): Is Stat3 and/or p53 mRNA expression a prognostic marker for renal cell carcinoma? Biomed. Res. **30,** 171-176 https://doi.org/10.2220/biomedres.30.171

Mattila KE, Laajala TD, Tornberg SV, Kilpeläinen TP, Vainio P, Ettala O, Boström PJ, Nisen H, Elo LL, Jaakkola PM (2021): A three-feature prediction model for metastasis-free survival after surgery of localized clear cell renal cell carcinoma. Sci. Rep. **11,** 8650 https://doi.org/10.1038/s41598-021-88177-9

Mishra A, Sullivan L, Caligiuri MA (2014): Molecular pathways: Interleukin-15 signaling in health and in cancer. Clin. Cancer Res. **20,** 2044-2050 https://doi.org/10.1158/1078-0432.CCR-12-3603

Mizoguchi A (2012): Animal models of inflammatory bowel disease. Prog. Mol. Biol. Transl. Sci. **105,** 263-320 https://doi.org/10.1016/B978-0-12-394596-9.00009-3

Motoshima T, Komohara Y, Horlad H, Tsukamoto H, Fujita M, Saito Y, Tanoue K, Kasejima Y, Sugiyama Y, Kawano Y, et al. (2016): CXCL10 and CCL2 mRNA expression in monocytes is inversely correlated with the HLA-DR lower fraction of monocytes in patients with renal cell carcinoma. Oncol. Lett. **11,** 1911-1916 https://doi.org/10.3892/ol.2016.4132

Nagarsheth N, Wicha MS, Zou W (2017): Chemokines in the cancer microenvironment and their relevance in cancer immunotherapy. Nat. Rev. Immunol. **17,** 559-572 https://doi.org/10.1038/nri.2017.49

Najjar YG, Rayman P, Jia X, Pavicic PG, Rini BI, Tannenbaum C, Ko J, Haywood S, Cohen P, Hamilton T, et al. (2017): Myeloid-derived suppressor cell subset accumulation in renal cell carcinoma parenchyma is associated with intratumoral expression of IL1β, IL8, CXCL5, and Mip-1α. Clin. Cancer Res. **23,** 2346-2355 https://doi.org/10.1158/1078-0432.CCR-15-1823

Negrier S, Perol D, Menetrier-Caux C, Escudier B, Pallardy M, Ravaud A, Douillard JY, Chevreau C, Lasset C, Blay JY (2004): Interleukin-6, Interleukin-10, and vascular endothelial growth factor in metastatic renal cell carcinoma: prognostic value of interleukin-6-from the Groupe Français d'Immunothérapie. J. Clin. Oncol. **22,** 2371-2378 https://doi.org/10.1200/JCO.2004.06.121

Nguyen KG, Vrabel MR, Mantooth SM, Hopkins JJ, Wagner ES, Gabaldon TA, Zaharoff DA (2020): Localized interleukin-12 for cancer immunotherapy. Front. Immunol. **11,** 575597 https://doi.org/10.3389/fimmu.2020.575597

Ntanasis-Stathopoulos I, Fotiou D, Terpos E (2020): CCL3 signaling in the tumor microenvironment. Adv. Exp. Med. Biol. **1231,** 13-21 https://doi.org/10.1007/978-3-030-36667-4_2

Oft M (2014): IL-10: Master switch from tumor-promoting inflammation to antitumor immunity. Cancer Immunol. Res. **2,** 194-199 https://doi.org/10.1158/2326-6066.CIR-13-0214

Padala SA, Barsouk A, Thandra KC, Saginala K, Mohammed A, Vakiti A, Rawla P, Barsouk A (2020): Epidemiology of renal cell carcinoma. World J. Oncol. **11,** 79-87 https://doi.org/10.14740/wjon1279

Pitarresi JR, Liu X, Sharma SM, Cuitiño MC, Kladney RD, Mace TA, Donohue S, Nayak SG, Qu C, Lee J, et al. (2016): Stromal ETS2 regulates chemokine production and immune cell recruitment during acinar-to-ductal metaplasia. Neoplasia **18,** 541-552 https://doi.org/10.1016/j.neo.2016.07.006

Polimeno M, Napolitano M, Costantini S, Portella L, Esposito A, Capone F, Guerriero E, Trotta A, Zanotta S, Pucci L, et al. (2013): Regulatory T cells, interleukin (IL)-6, IL-8, vascular endothelial growth factor (VEGF), CXCL10, CXCL11, epidermal growth factor (EGF) and hepatocyte growth factor (HGF) as surrogate markers of host immunity in patients with renal cell carcinoma. BJU International **112,** 686-696 https://doi.org/10.1111/bju.12068

R Core Team (2021): A language and environment for statistical computing. R Foundation for Statistical Computing

Santoni M, Conti A, Piva F, Massari F, Ciccarese C, Burattini L, Cheng L, Lopez-Beltran A, Scarpelli M, Santini D, et al. (2015): Role of STAT3 pathway in genitourinary tumors. Future Sci. OA **1,** FSO15 https://doi.org/10.4155/fso.15.13

Sato E, Fujimoto J, Tamaya T (2007): Expression of interferon-gamma-inducible protein 10 related to angiogenesis in uterine endometrial cancers. Oncology **73,** 246-251 https://doi.org/10.1159/000127422

Shanmugam MK, Rajendran P, Li F, Kim C, Sikka S, Siveen KS, Kumar AP, Ahn KS, Sethi G (2015): Abrogation of STAT3 signaling cascade by zerumbone inhibits proliferation and induces apoptosis in renal cell carcinoma xenograft mouse model. Mol. Carcinog. **54,** 971-985 https://doi.org/10.1002/mc.22166

Sinha P, Clements VK, Ostrand-Rosenberg S (2005): Interleukin-13-regulated M2 macrophages in combination with myeloid suppressor cells block immune surveillance against metastasis. Cancer Res. **65,** 11743-11751 https://doi.org/10.1158/0008-5472.CAN-05-0045

Srabovic N, Mujagic Z, Mujanovic-Mustedanagic J, Muminovic Z, Softic A, Begic L (2011): Interleukin 13 expression in the primary breast cancer tumor tissue. Biochem. Med. **21,** 131-138 https://doi.org/10.11613/BM.2011.021

Suyama T, Furuya M, Nishiyama M, Kasuya Y, Kimura S, Ichikawa T, Ueda T, Nikaido T, Ito H, Ishikura H (2005): Up-regulation of the interferon γ (IFN-γ)-inducible chemokines IFN-inducible T-cell α chemoattractant and monokine induced by IFN-γ and of their receptor CXC receptor 3 in human renal cell carcinoma. Cancer **103,** 258-267 https://doi.org/10.1002/cncr.20747

Takenawa J, Kaneko Y, Fukumoto M, Fukatsu A, Hirano T, Fukuyama H, Nakayama H, Fujita J, Yoshida O (1991): Enhanced expression of interleukin-6 in primary human renal cell carcinomas. J. Natl. Cancer Inst. **83,** 1668-1672 https://doi.org/10.1093/jnci/83.22.1668

Tang Z, Li C, Kang B, Gao G, Li C, Zhang Z (2017): GEPIA: a web server for cancer and normal gene expression profiling and interactive analyses. Nucleic Acids Res. **45,** W98-W102 https://doi.org/10.1093/nar/gkx247

Tugues S, Burkhard SH, Ohs I, Vrohlings M, Nussbaum K, vom Berg J, Kulig P, Becher B (2015): New insights into IL-12-mediated tumor suppression. Cell Death Differ. **22,** 237-246 https://doi.org/10.1038/cdd.2014.134

Urdinguio RG, Fernandez AF, Moncada-Pazos A, Huidobro C, Rodriguez RM, Ferrero C, Martinez-Camblor P, Obaya AJ, Bernal T, Parra-Blanco A, et al. (2013): Immune-dependent and independent antitumor activity of GM-CSF aberrantly expressed by mouse and human colorectal tumors. Cancer Res. **73,** 395-405 https://doi.org/10.1158/0008-5472.CAN-12-0806

Utsumi T, Suyama T, Imamura Y, Fuse M, Sakamoto S, Nihei N, Ueda T, Suzuki H, Seki N, Ichikawa T (2014): The association of CXCR3 and renal cell carcinoma metastasis. J. Urol. **192,** 567-574 https://doi.org/10.1016/j.juro.2014.01.100

Vargová D, Ľupták J, Dargaj J, Fraňová S, Kocmálová M, Šutovský J, Švihra J, Škorňová I, Slávik P, Grendár M (2022): Cytokines

in renal cell carcinoma: A step towards earlier detection and targeted therapy. Adv. Exp. Med. Biol. **1374,** 63-72 https://doi.org/10.1007/5584_2021_700

Verhoeven Y, Tilborghs S, Jacobs J, de Waele J, Quatannens D, Deben C, Prenen H, Pauwels P, Trinh XB, Wouters A, et al. (2020): The potential and controversy of targeting STAT family members in cancer. Semin. Cancer Biol. **60,** 41-56 https://doi.org/10.1016/j.semcancer.2019.10.002

Vuong L, Kotecha RR, Voss MH, Hakimi AA (2019): Tumor microenvironment dynamics in clear-cell renal cell carcinoma. Cancer Discov. **9,** 1349-1357 https://doi.org/10.1158/2159-8290.CD-19-0499

Wang W, Qi L, Tan M, Zhang Z, Du J, Wei X, Yao X (2015): Effect of platelet-derived growth factor-B on renal cell carcinoma growth and progression. Urol. Oncol. **33,** 168e17-168e27 https://doi.org/10.1016/j.urolonc.2014.12.015

Wightman SC, Uppal A, Pitroda SP, Ganai S, Burnette B, Stack M, Oshima G, Khan S, Huang X, Posner MC, et al. (2015): Oncogenic CXCL10 signalling drives metastasis development and poor clinical outcome. Br. J. Cancer **113,** 327-335 https://doi.org/10.1038/bjc.2015.193

Xin H, Zhang C, Herrmann A, Du Y, Figlin R, Yu H (2009): Sunitinib inhibition of Stat3 induces renal cell carcinoma tumor cell apoptosis and reduces immunosuppressive cells. Cancer Res. **69,** 2506-2513 https://doi.org/10.1158/0008-5472.CAN-08-4323

Zhang S, Zhang E, Long J, Hu Z, Peng J, Liu L, Tang F, Li L, Ouyang Y, Zeng Z (2019): Immune infiltration in renal cell carcinoma. Cancer Sci. **110,** 1564-1572 https://doi.org/10.1111/cas.13996

Zhao J, Zhao J, Perlman S (2012): Differential effects of IL-12 on Tregs and Non-Treg T Cells: Roles of IFN-γ, IL-2 and IL-2R. PLoS One **7,** e46241 https://doi.org/10.1371/journal.pone.0046241

Zou S, Tong Q, Liu B, Huang W, Tian Y, Fu X (2020): Targeting STAT3 in cancer immunotherapy. Mol. Cancer **19,** 145 https://doi.org/10.1186/s12943-020-01258-7

Received: January 18, 2023
Final version accepted: May 26, 2023

doi: 10.4149/gpb_2023015

Supplementary Material

Immunobiochemical profile of clear cell renal cell carcinoma (ccRCC): A preliminary study

Daniela Vargová[1], Ján Dargaj[2], Soňa Fraňová[1], Matúš Dohál[3], Ján Ľupták[2], Ján Švihra[2], Lukáš Briš[2], Marián Grendár[4] and Martina Šutovská[1]

[1] *Department of Pharmacology, Jessenius Faculty of Medicine in Martin, Comenius University in Bratislava, Martin, Slovakia*
[2] *Department of Urology, Jessenius Faculty of Medicine in Martin, Comenius University in Bratislava and University Hospital Martin, Slovakia*
[3] *Biomedical Centre Martin, Jessenius Faculty of Medicine in Martin, Comenius University in Bratislava, Martin, Slovakia*
[4] *Bioinformatic unit, Biomedical Center Martin, Jessenius Faculty of Medicine in Martin, Comenius University in Bratislava, Martin, Slovakia*

Table S1. Expression of cytokine and STAT3 genes in ccRCC compared to healthy kidney tissue

Gene name (Cytokine name)	Median Gene Expression[1] (N)		
	ccRCC (523)	Normal (100)	Significance[2]
CSF3 (G-CSF)	0.04	0.08	ns
CSF2 (GM-CSF)	0.04	0	
IL6	1.69	1.77	
IL7	1.98	1.07	
IL10	0.85	0.3	
IL12A (IL-12p70)	0.32	0.32	
IL12B (IL-12p70)	0.08	0.03	
IL13	0.04	0	
CXCL10	4.67	1.9	*
CCL3	3.71	1.89	*
CCL4	4.44	2.1	*
STAT3	0.04	0.08	ns
FGF2 (bFGF)	2.19	2.33	
IFNG	0.41	0.04	
IL1B	2.22	1.53	
IL1RN (IL-1ra)	1.34	1.06	
IL2	0.1	0	
IL4	0	0	
IL5	0.04	0	
CXCL8 (IL-8)	1.82	2.01	
IL9	0	0	
IL15	2.95	2.3	
IL17	0	0	
CCL2	6.96	6.48	
RANTES/CCL5	5.52	2.49	
TNF	0.54	0.51	
VEGF	9.63	6.17	*
CXCL11 (EOTAXIN)	2.21	0.38	*
PDGFB	4.63	3.91	ns

The table shows a summary of median expression values of 28 genes in clear cell renal cell carcinoma (ccRCC) compared to healthy kidney tissue (Normal). Data were obtained from the selected data sets 'TCGA tumors *vs.* TCGA normal + GTEx normal'. The differential analysis was performed using the interactive online web server GEPIA (Tang et al. 2017). The median expressions (transcripts *per* million – TPM) are on a logarithmic scale (Log2(TPM+1)); [1] fold-change threshold ($|\log_2 FC|$) was established at 1.0; [2] *p* value cutoff was established at 0.05; ns, not significant; N, number of samples.